APOLLO LUNAR MODULE VIBRATIONS DURING FLIGHT AND GROUND TESTS

Wade D. Dorland and James D. Johnston, Jr.
NASA Manned Spacecraft Center
Houston, Texas

The development of the Apollo lunar module provided a unique opportunity to compare payload vibration during launch and during acoustic-ground-test simulations of launch-pad booster noise. In the course of structural development of the lunar module, vibration measurements were made at identical locations on both the ground-test lunar module (lunar module test article number 3) and the first two flight vehicles, lunar module 1 launched in the Apollo 5 mission and lunar module 3 launched in the Apollo 9 mission. Sound-level measurements were also recorded both in the ground tests and during launch of lunar module mockups on Saturn V boosters 501 and 502. Evaluation of these launch and ground-test vibration data yields comparisons which are particularly useful because the vehicles were highly similar and because sufficient data were available to be statistically meaningful. A rigorous examination of laboratory/flight comparisons, which was thereby made possible and is discussed in detail in this paper, shows the promise (and compromise) in ground-test simulation of flight responses.

INTRODUCTION

The engineering development of the Apollo lunar module (LM) involved a wide spectrum of analyses and tests to assure that the LM structure could perform the necessary functions through all phases of the mission. In particular, because structural adequacy is required for the high-frequency environmental excitations (over 25 Hz), an acoustic test program in which flight environments were simulated as closely as possible was conducted before the first LM flight to demonstrate a sufficient structural margin. Subsequently, two LM vehicles (one unmanned and one manned) were flown to prove the functional adequacy of the structure and of all other vehicle systems. These flights provided vibration data that could be directly compared with the ground-test data. The similarity of the data from the ground and flight tests would indicate the extent of flight simulation obtained in the ground test. In the LM program, however, the flight vibration data were not very similar to the ground-test vibration data. The data dissimilarities are attributed to structural complexity and instrumentation differences and preclude detailed assessment of the fidelity of ground test simulation.

The purposes of this paper are to describe and evaluate the LM vibrations measured in both the ground and the flight tests relevant to an assessment of acoustic testing effectiveness and to make recommendations for future testing programs.

LUNAR MODULE VEHICLE AND ENVIRONMENT

An understanding of the LM vehicle and its flight environment will readily lead to a discussion of the vibration environment. The LM vehicle (Figs. 1 and 2) consists of a descent stage and a separate ascent stage interconnected at four points. The basic descent-stage structure (Fig. 3) is a 65-in.-deep cruciform consisting of a central engine compartment and four propellant-tank compartments. Each of the four landing-gear legs is mounted on an outrigger assembly which also

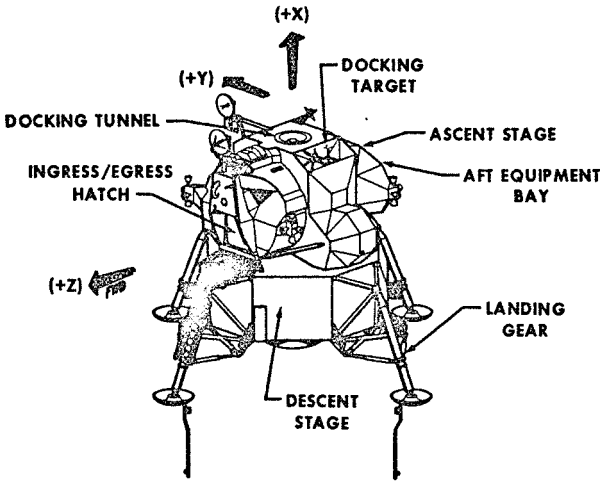

Figure 1. - Lunar landing configuration of Apollo lunar module

serves as a support when the vehicle is inside the service module LM adapter (SLA). Auxiliary equipment, such as the helium and oxygen tanks and the Apollo lunar-surface exploration package, is mounted in the four quadrants of the descent-stage cruciform. The ascent stage (Fig. 4) consists of two cylindrical sections capped by forward and aft machined bulkheads; a major intermediate bulkhead separates the crew area from the aft cabin. The primary load-carrying structural elements of both stages are thin-webbed (typically less than 0.020 inch thick) shear panels with integral stiffeners along all four edges. Under load, visible buckle patterns occur in these shear panels. Since the buckle patterns vary considerably with load (static, dynamic, or combined) and dimensional variations from vehicle to vehicle, the influence of these buckle patterns on LM structural dynamics is also

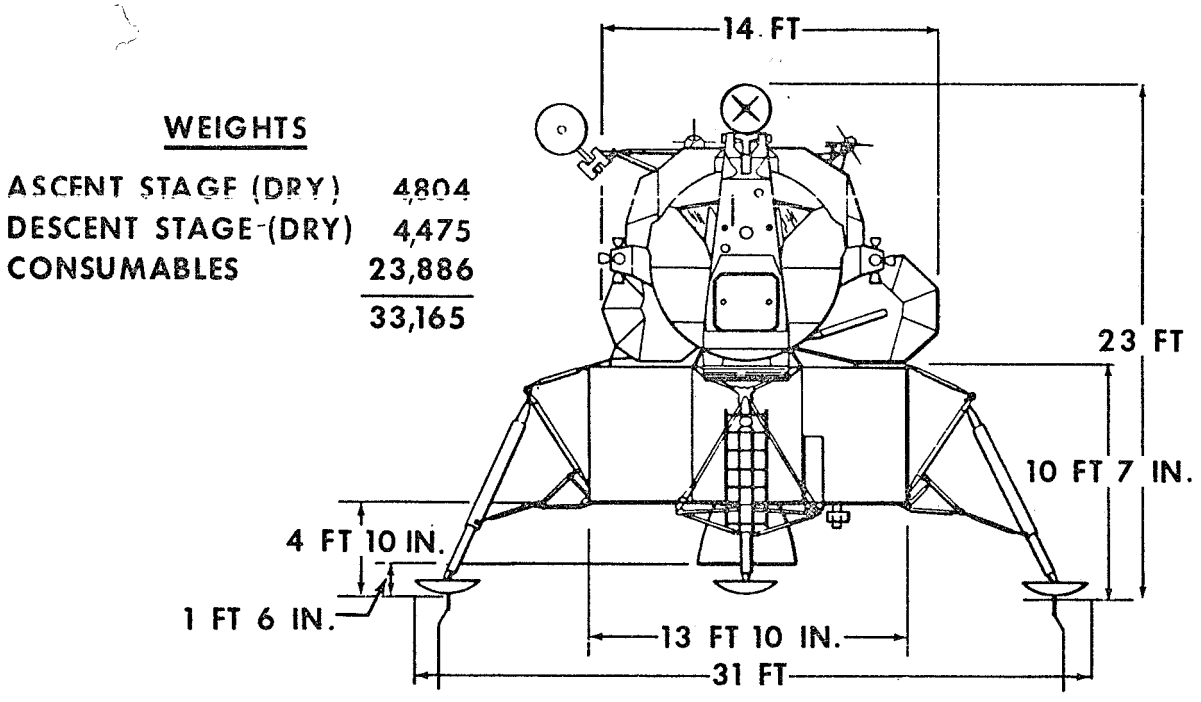

Figure 2. - Lunar module weights and dimensions

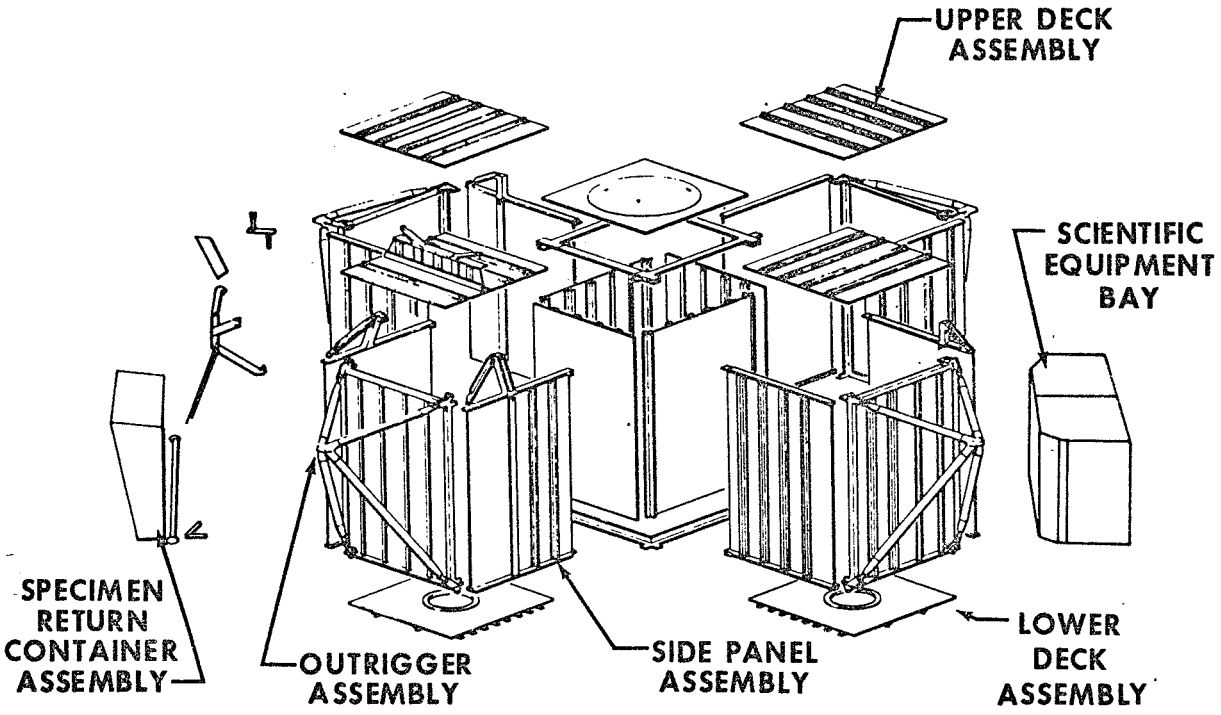

Figure 3.- Lunar module descent-stage structure

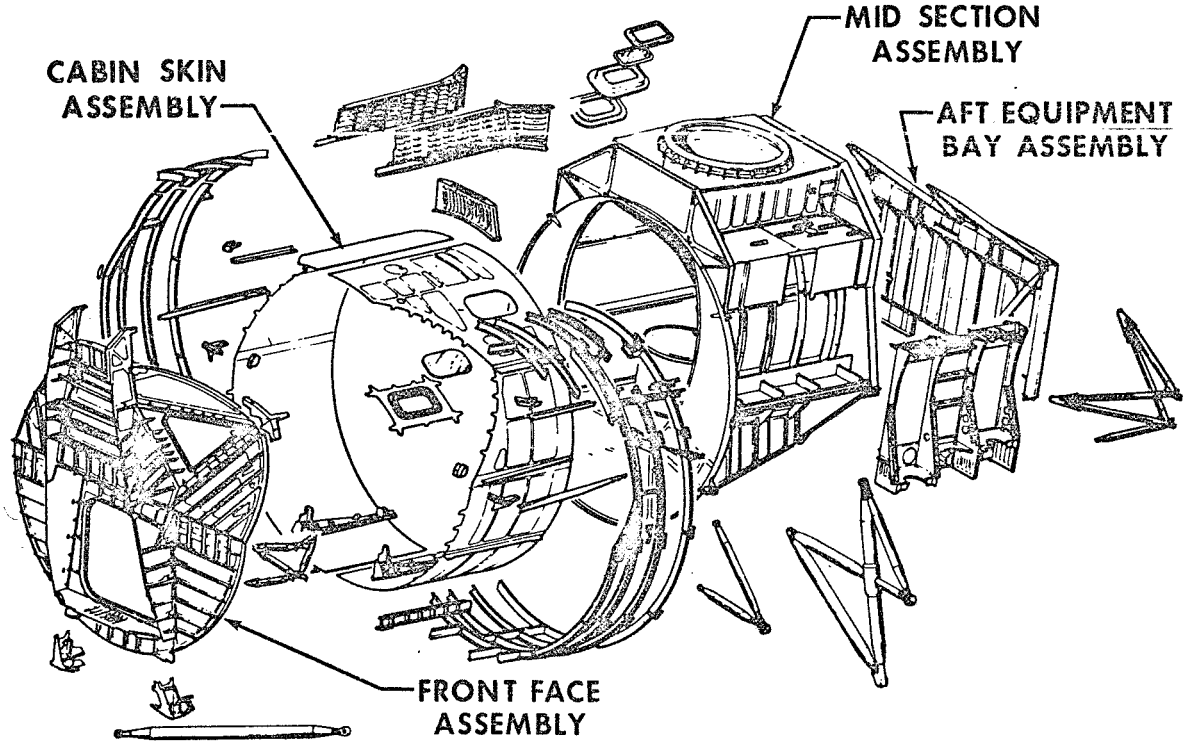

Figure 4.- Lunar module ascent-stage structure

highly variable from vehicle to vehicle. The ascent engine is mounted from the midsection floor. Two spherical propellant tanks are supported from the bulkheads, primarily by struts. Much of the electronic equipment is located in the aft equipment bay and is mounted on a vertical rack supported by struts that extend from the rear bulkhead.

During the initial phase of an Apollo mission, the LM is located in the SLA (Fig. 5). The SLA is a 28-ft-long truncated cone that fairs the command module and the service module parts of the space vehicle into the Saturn-IVB (S-IVB) stage. The S-IVB stage can be either the second stage of a Saturn-IB (S-IB) or a Saturn-V (S-V) booster depending on the mission objectives. The LM is exposed to both low-frequency mechanical vibration and high-frequency acoustic excitation at liftoff and during atmospheric flight. Mechanically induced vibration transmitted from the SLA panels through the support trusses is limited to low-frequency vibrations. For vibration transmissibility above 12 Hz, the LM vehicle is effectively decoupled from the SLA and experiences only high-frequency acoustic excitation. The induced high-frequency vibration of the LM is closely related to the internal acoustic environment of the SLA. The associated noise levels follow the typical rocket booster flight profile (Fig. 6) of decreasing rapidly after liftoff and then increasing to a peak near Mach 1. The external noise levels induce vibration of the SLA panels, generating a quasi-reverberant acoustic field inside the SLA. The internal SLA noise is

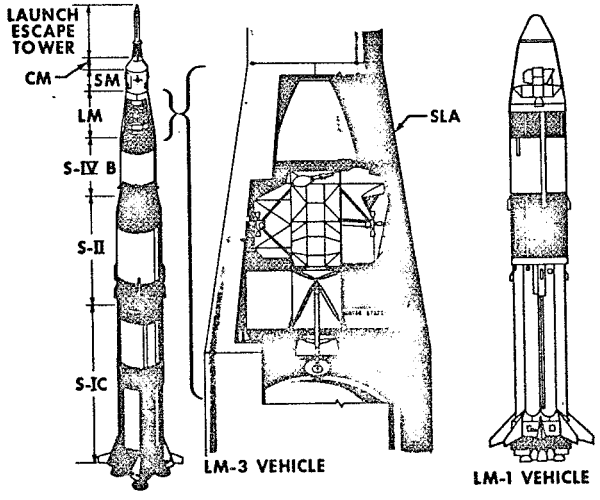

Figure 5. - Apollo/Saturn space vehicles

considered to be the most significant source of LM excitation and follows the profile shown in Fig. 6.

A LM vehicle built specifically for structural ground testing and designated LM Test Article number 3 (LTA-3) was used for the acoustic ground test. The LTA-3 was a complete structural demonstrator with an unabridged complement of prototype or mass-representative equipment and subsystems. All fluid tanks were ballasted to the control weight with either water or Freon 113 to obtain the correct mass loads (Fig. 2) in the structure. A more detailed description of LTA-3 is contained in Refs. [1] and [2]. The primary structural elements of LTA-3 and of all other LM test articles are shown in Figs. 3 and 4.

INSTRUMENTATION AND MEASUREMENT

A discussion of the instrumentation and relevant measurements and a description of the test programs will provide the information necessary for evaluation of the LM vibration data.

Vibration Measurements

The LM vehicles launched in the flight-test program were the unmanned LM-1 (Apollo 4 mission, S-IB booster number 204) and the manned LM-3 (Apollo 9 mission, S-V booster number 503). The launch configurations for both flights are shown in Fig. 5. The LM-1 and LM-3 vehicles each had 26 vibration-measurement sensors mounted at identical selected locations. Of these sensors, the 16 that produced pertinent vibration data were five triaxial installations and one X-axis-oriented sensor. The relative locations of the sensors and the measurement numbers are given in Fig. 7. The high degree of similarity between the instrumentation installations on LTA-3, LM-1, and LM-3 can be seen in Figs. 8, 9, and 10 which show the details of the installations on each vehicle for three typical locations. The similarity of the other locations was equally good but the photographic documentation was not as clear.

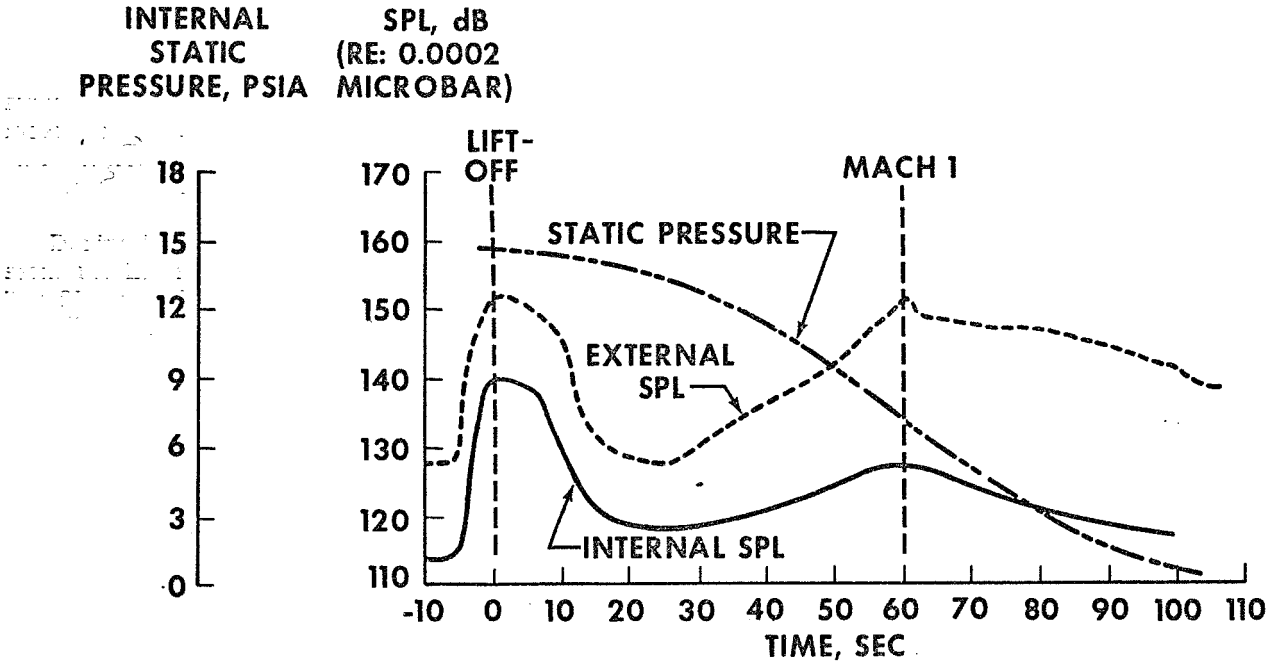

Figure 6. - Typical profiles of SLA sound levels and internal static pressure during the initial 100 sec of launch and boost

LOCATION NO.	MEASUREMENT NO.	LOCATION DESCRIPTION
1	6001 (Z) 6002 (Y) 6003 (X)	NAVIGATION BASE
2	3661 (X) 3662 (Y) 3663 (Z)	TUNNEL EQUIPMENT AREA
3	3601 (X) 3602 (Y) 3603 (Z)	AFT EQUIPMENT RACK
4	1571 (X) 1572 (Y) 1573 (Z)	ASCENT-STAGE OXIDIZER TANK
5	2681 (X) 2682 (Y) 2683 (Z)	DESCENT-STAGE OXIDIZER TANK (-Z-AXIS)
6	7559 (X)	LANDING RADAR ANTENNA

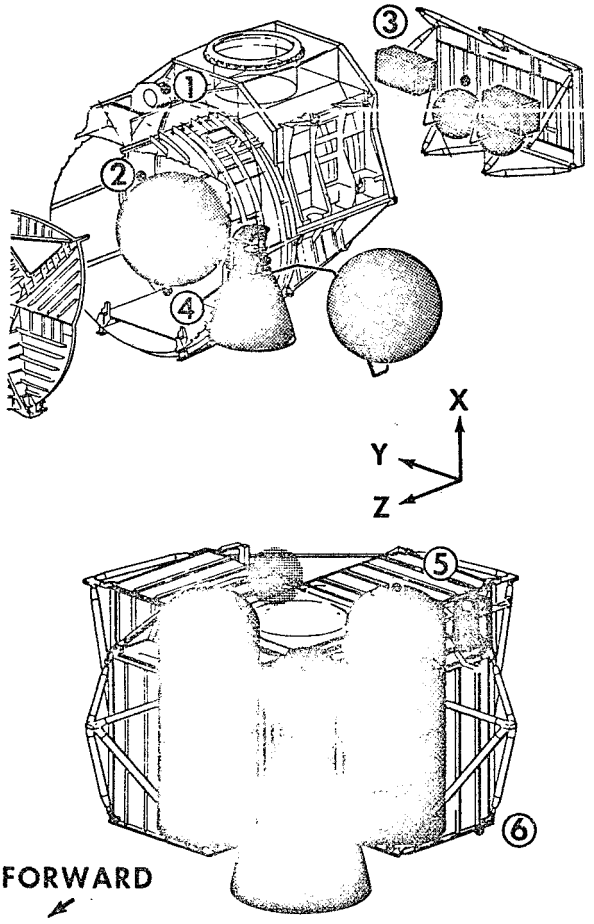

Figure 7. - Lunar module instrumentation locations

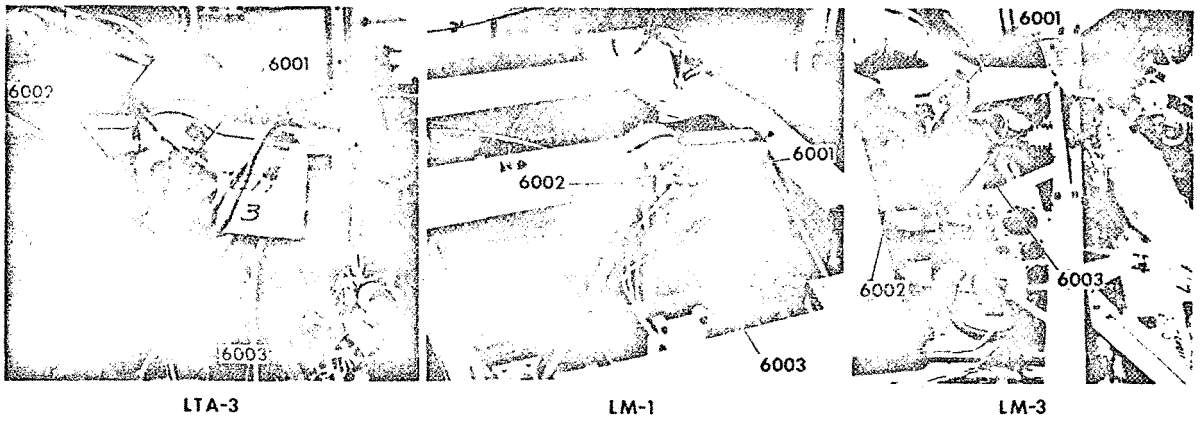

Figure 8. - Accelerometer installation on navigation base (see Fig. 7, location no. 1)

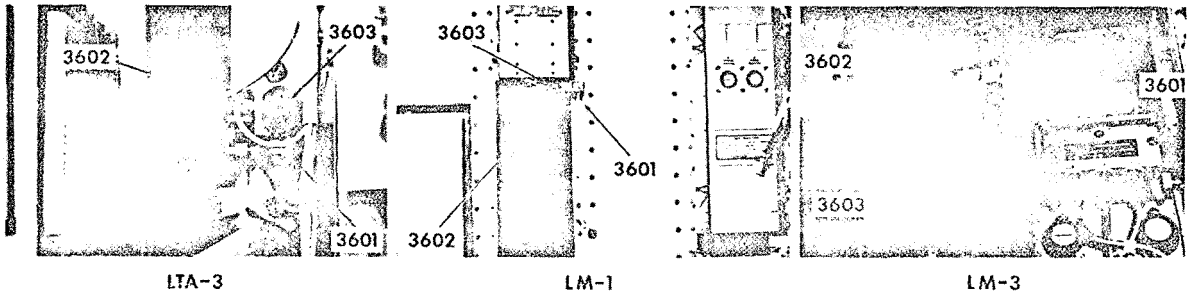

Figure 9. - Accelerometer installation on aft equipment rack (see Fig. 7, location no. 3)

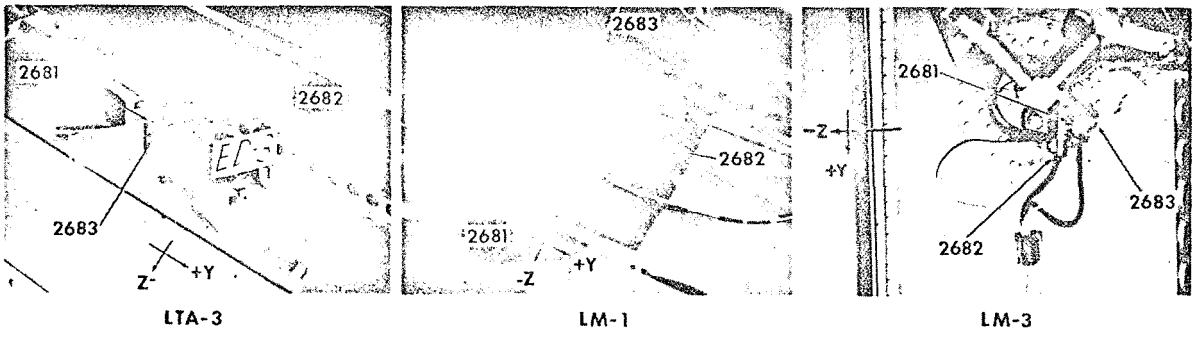

Figure 10. - Accelerometer installation on descent-stage oxidizer tank (see Fig. 7, location no. 5)

The LTA-3 measurements were made at locations identical to those of the aforementioned flight measurements. Although data on all three vehicles were obtained with piezoelectric accelerometers and associated charge amplifiers, different recording systems were used. The LTA-3 data were recorded on constant-bandwidth frequency-modulation (FM) and FM-multiplex tape recorders which met high laboratory performance standards. The flight data were telemetered from the vehicle to a ground station through a complex radio-frequency link and then recorded. Because of the complexity of the flight data system (i. e., narrower bandwidths and dynamic ranges), fewer data were obtained for LM-1 and LM-3 than for LTA-3. Data-acquisition information on these measurements is given in Table 1.

TABLE 1
Data Acquisition Information

Location		Measurement No.	Range (g peak)		Useful Data Bandwidth (Hz)		
No.	Description		LTA-3	LM-1 and LM-3	LTA-3	LM-1	LM-3
1	Navigation base	[a]6001 (Z)	±24	±2	2500	2000	2000
		6002 (Y)	±24	±2	2500	2000	2000
		6003 (X)	±24	±2	2500	2000	2000
2	Tunnel equipment area	3661 (X)	±30	±30	2500	2000	[b]2000
		3662 (Y)	±8	±30	2500	2000	[b]2000
		3663 (Z)	±8	±30	2500	2000	[b]2000
3	Aft equipment rack	3601 (X)	±3.16	±20	2500	1000	600
		3602 (Y)	±10	±20	2500	1000	600
		3603 (Z)	±10	±20	2500	1000	600
4	Ascent-stage oxidizer tank	1571 (X)	±10	±10	2500	[b]175	[b]160
		1572 (Y)	±10	±10	2500	125	110
		1573 (Z)	±10	±10	2500	125	110
5	Descent-stage oxidizer tank (-Z-axis)	2681 (X)	±10	±10	2500	[b]125	[b]110
		2682 (Y)	±10	±10	2500	125	110
		2683 (Z)	±10	±10	2500	125	110
6	Landing radar antenna	7559 (X)	±24	±10	2500	125	110

[a]Because of confusion in nomenclature between the structure and the guidance and navigation subsystem, the numbering order of the 6000-series triax was inadvertently reversed.

[b]These measurements were telemetered continuously; all other measurements were arranged in groups of three on a slow-speed commutator that commutated the measurements sequentially to the telemetry system with a switch rate of 1.25 sec. Hence, the measurements were recorded for 1.25 sec then blanked for 2.5 sec, then recorded and so on. The switching time of the commutator was 50 msec.

The raw data for all measurements were random in nature and, therefore, power spectral density (PSD) processing was performed on these measurements. The processing parameters were selected to obtain the minimum statistical error commensurate with data stationarity and commutator operation. However, the only significant responses which LM-1 and LM-3 exhibited during the first stage of powered flight occurred at liftoff, and, therefore, only these data are comparable to the ground-test data on the LTA-3 responses. The pertinent data-reduction information is presented in Table 2.

Sound Measurements

Two sound measurements inside the SLA were recorded during each of the first two flights of the S-V booster. During the LTA-3 acoustic testing, the initial objective was to have sound-measurement sensors placed in identical locations; however, physical constraints precluded this. Six measurement sensors thus were placed in locations near the locations of the flight sensors (Fig. 11) and pertinent data were measured. The LTA-3 sound data-acquisition equipment was identical to the vibration data-acquisition equipment except for the functional difference in the sensors

(piezoelectric microphones were used to obtain the sound data). The same similarity applied to the flight data. Specific information on the acquisition and processing of the sound measurements is given in Table 3.

TABLE 2
Data Reduction Information

Location		Measurement No.	Slice Time (sec)[a]			Processing Bandwidth (Hz)			PSD Processing Degrees of Freedom		
No.	Description		LTA-3	LM-1	LM-3	LTA-3	LM-1	LM-3	LTA-3	LM-1	LM-3
1	Navigation base	[b]6001 (Z)	10.0 to 17.8	2.00 to 3.00	3.10 to 4.10	8.062	8.000	6.092	126	16	12
		6002 (Y)	10.0 to 17.8	No data	1.80 to 2.80	8.062	8.000	6.092	126	16	12
		6003 (X)	10.0 to 17.8	0.50 to 1.50	0.50 to 1.50	8.063	8.000	6.092	126	16	12
2	Tunnel equipment area	3661 (X)	10.0 to 17.8	1.65 to 2.65	0.00 to 2.00	8.055	8.000	6.092	126	16	24
		3662 (Y)	10.0 to 17.8	-1.00 to 0	0.00 to 2.00	8.071	8.000	6.095	126	16	24
		3663 (Z)	10.0 to 17.8	0.30 to 1.30	0.00 to 2.00	8.071	8.000	6.095	126	16	24
3	Aft equipment rack	3601 (X)	10.0 to 17.8	2.00 to 3.00	1.80 to 2.80	8.063	6.000	6.093	126	12	12
		3602 (Y)	10.0 to 17.8	-0.75 to 0.25	3.10 to 4.10	8.063	6.000	6.093	126	12	12
		3603 (Z)	10.0 to 17.8	0.50 to 1.50	0.50 to 1.50	8.063	6.000	6.097	126	12	12
4	Ascent-stage oxidizer tank	1571 (X)	10.0 to 17.8	-1.65 to 0.35	0.00 to 2.00	8.055	6.000	6.093	126	24	24
		1572 (Y)	10.0 to 17.8	-1.50 to -0.50	3.10 to 4.10	8.055	6.000	6.338	126	12	13
		1573 (Z)	10.0 to 17.8	-1.50 to 0.50	3.10 to 4.10	8.055	6.000	6.338	126	12	13
5	Descent-stage oxidizer tank	2681 (X)	10.0 to 17.8	-1.65 to 0.35	0.00 to 2.00	8.055	6.000	6.093	126	24	24
		2682 (Y)	10.0 to 17.8	-0.20 to 0.80	0.50 to 1.50	8.062	6.000	6.332	126	12	13
		2683 (Z)	10.0 to 17.8	-0.20 to 0.80	0.50 to 1.50	8.062	6.000	6.338	126	12	13
6	Landing radar antenna	7559 (X)	10.0 to 17.8	1.10 to 2.10	1.80 to 2.80	8.055	6.000	6.338	126	12	13

[a]The LTA-3 slice time is the time after the start of the test during which the data were strongly stationary from +1 sec to the end of the test. The LM-1 and LM-3 slice times are the number of seconds before (-) or after (no sign) range zero, which is defined as the start of the first integral second after initial motion of the booster.

[b]Because of a confusion in nomenclature between the structure and the guidance and navigation subsystem, the numbering order of the 6000-series triax was inadvertently reversed.

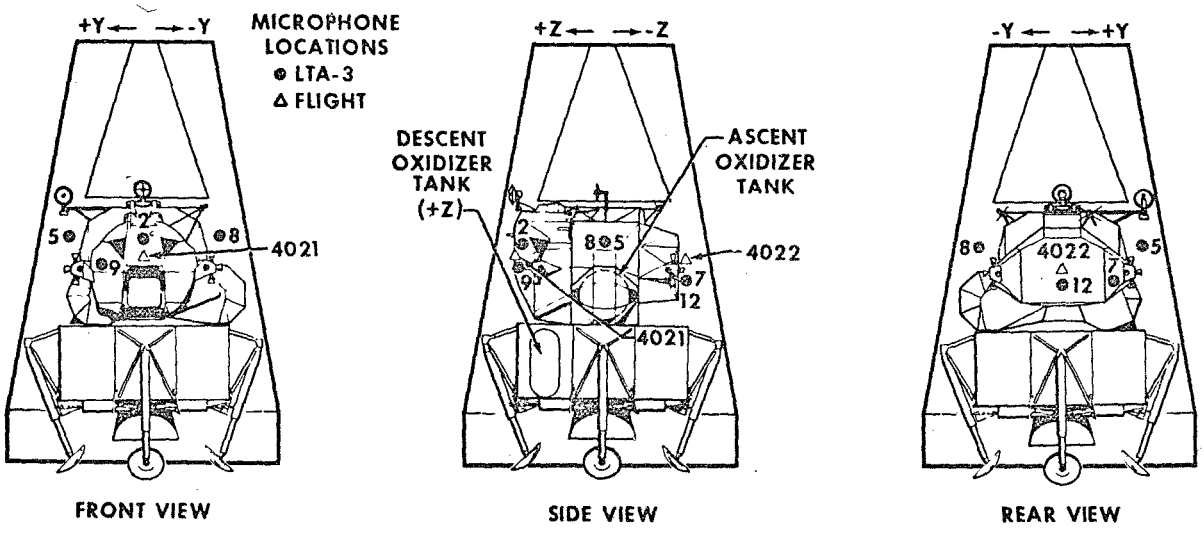

Figure 11.- Sound-measurement locations inside the SLA

TABLE 3
Sound Measurement Acquisition and Processing Information

Parameter	Flight Data	Ground-Test Data
Measurement number	4021 and 4022	Internal microphone nos. 2, 5, 7, 8, 9, and 12
Useful data bandwidth (Hz)	2000	2500
SPL range (dB)	150 maximum	150 maximum
Slice time (sec)	-1.0 to +1.0	10.0 to 18.0
Processing bandwidth (Hz)	8.01	8.063
PSD processing degrees of freedom	32	128

ACOUSTIC GROUND-TEST PROGRAM

The acoustic ground testing of the LM is described extensively in Refs. [1] and [2]. The acoustic testing levels and duration were specified to envelop all dynamic (acoustic or aerodynamic) pressure levels that were expected during launches from either S-IB or S-V boosters. Based on flight data from Apollo/Saturn missions 201 and 202, liftoff noise controlled the spectral levels in the 1/3-octave bands between 50 and 400 Hz; transonic noise levels were slightly higher in the other bands. The LTA-3 vehicle successfully withstood 2-1/2 min of excitation applied in eight successive runs. Measured sound and vibration levels were highly repeatable from run to run; therefore, the data obtained from the LTA-3 test series were considered to be highly reliable and uncompromised in any significant respect.

FLIGHT-TEST PROGRAM

The LM-1 vehicle was launched by an S-IB booster on January 22, 1968; and all primary mission objectives were successfully completed. Although the LM-1 systems were fully functional, the LM-1 vehicle was flown unmanned, and a programer simulated the functional operations of the commander and the pilot. The LM-3 vehicle was launched by an S-V booster on March 3, 1969, and was successfully flown through all prescribed maneuvers by Astronauts McDivitt and Schweickart. Again, all mission objectives were met. The launch and boost phase of the flight profile was nominal, and no significant exceptions from the dynamic-pressure/time function given in Fig. 6 were experienced. Useful vibration data were obtained from both flights with only two measurement anomalies. The anomalies were the failure of LM-1 measurement sensor number 6002 (located on the Y-axis of the navigation base) and the invalidation of data from the triax on the aft equipment rack (sensor numbers 3601, 3602, and 3603) because of high-frequency noise above 600 Hz.

The sound measurements inside the SLA were made during the launches of S-V boosters 501 and 502 which also had completely nominal launch profiles. The SLA volumes on boosters 501 and 502 were occupied by LTA-2R and LTA-10R, respectively. The primary elements of the LTA-2R and LTA-10R configurations are shown in Fig. 12. Although these vehicles had reasonably accurate descent-stage structural simulators and volumes and masses representative of the ascent stage, neither vehicle had a thermal shield. The thermal shield is a resilient assembly composed of multiple layers of aluminized Mylar with a thin aluminum outer surface and can absorb considerable sound energy at some frequencies. The absence of a thermal shield on LTA-2R and LTA-10R could therefore substantially affect the characteristics of the sound field within the SLA volume and result in acoustic data unique to these two missions.

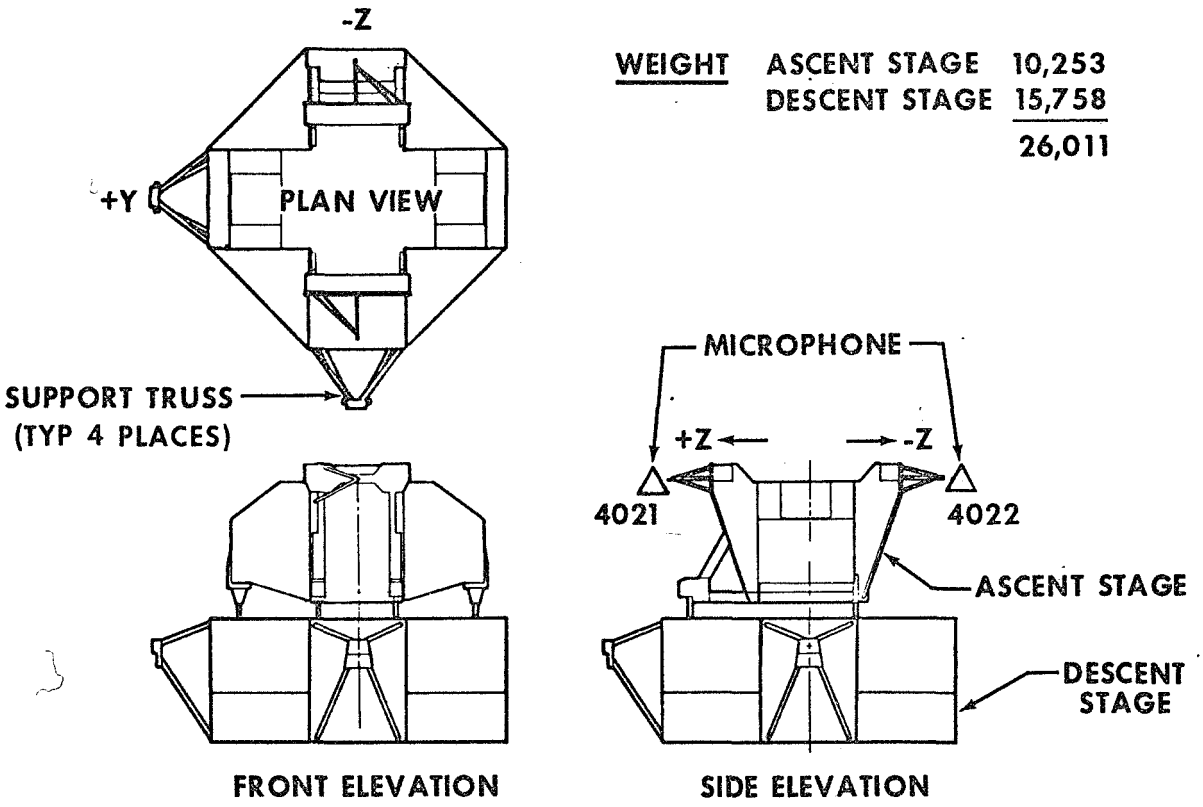

Figure 12. - Details of LTA-2R and LTA-10R

DATA PRESENTATION

Vibration Data

The individual measurements at each sensor location were compared, but few significant trends could be distinguished. The large statistical error in the processing of the flight data as indicated by the small value of the degrees of freedom (always less than 25) and the many small configuration differences between the vehicles evidently obscured all trends. Furthermore, the differences in the acoustic environments between the flight and the ground tests, while small, apparently were sufficient to make the comparisons enigmatic at best. Ensemble averaging to reduce statistical errors therefore appeared to have considerable merit [3]. The resulting averages were obtained for four groups and are listed in Table 4. The statistical error (ϵ) produced by ensemble averaging is sufficiently small to provide meaningful comparisons. The resulting ensemble average PSD for each group is plotted in Figs. 13 to 16, as listed in Table 4.

Sound Data

As described in the foregoing section on instrumentation and measurements, sound data were available from six ground test measurements and four flight test measurements located within the SLA. For an assessment of the similarity of the flight and ground test sound levels, the maximum and minimum values of the 1/3-octave-band SPL's (or range of data) can be compared. At lift-off, the range of flight data (solid lines in Fig. 17) and the range of ground test data (dashed lines) showed large areas of overlap or excellent agreement. However, during the transonic and max-Q excitation periods of the launch phase when significant excitation to the SLA exterior occurs, the internal sound and pressure levels (SPL) decreased more than 10 dB from the liftoff values (Fig. 6). This decrease can be attributed to the fact that the mass and density of the gas occupying the internal volume of the SLA had decayed sufficiently through venting to reduce significantly the joint acceptance of the fluid/structure interface of the SLA interior surface. The static pressure of the volume during this

TABLE 4
Ensemble Averaging Information

Group Designation	Figure No.	Measurement Nos.	Normalized Statistical Error (ϵ)		Description
			LTA-3	LM-1 and LM-3	
A	13	6003 3661 3601 7559	0.065	0.131	Longitudinal (X-axis) response of secondary structure (navigation base, tunnel equipment area, aft equipment rack, and landing radar antenna)
B	14	6001 6002 3662 3663 3602 3603	.053	.109	Lateral response of secondary structure
C	15	1571 1572 1573 2681 2682 2683 7559	.049	.095	Combined triaxial response of major mass items (tanks and descent-stage structure) below 110 Hz
D	16	1572 1573 2682 2683	.065	.142	Lateral response of tanks

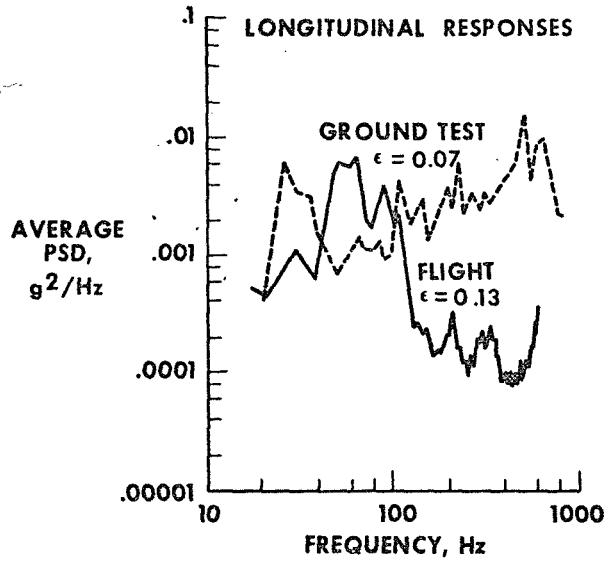

Figure 13. - Average vibration responses: Group A, longitudinal response (X-axis) of secondary structure

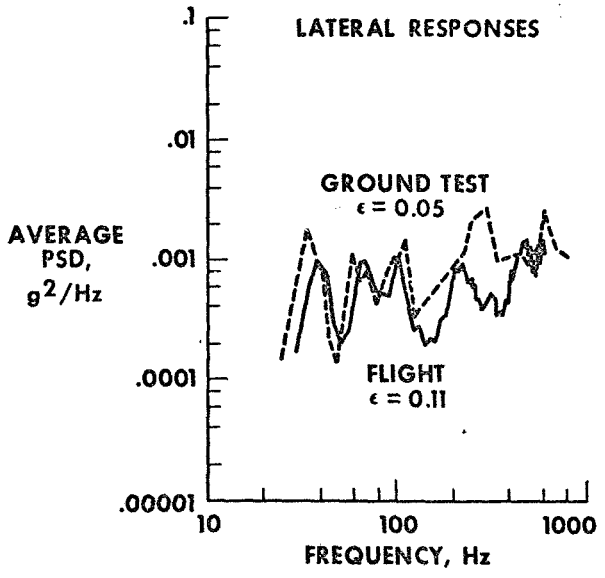

Figure 14. - Average vibration responses: Group B, lateral response (Y- and Z-axes) of secondary structure

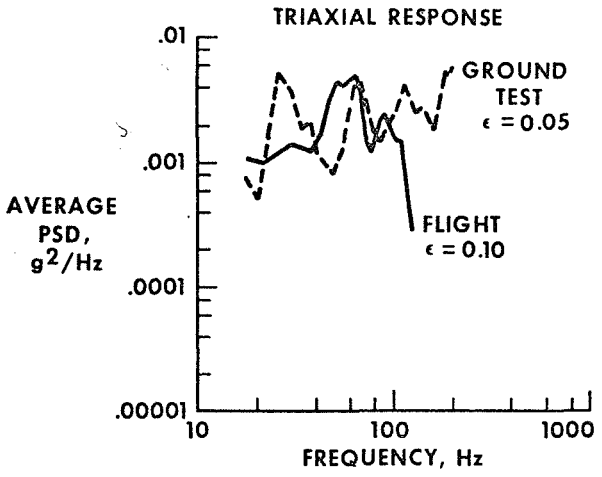

Figure 15. - Average vibration responses: Group C, combined triaxial response of major mass items (tanks and descent-stage structure)

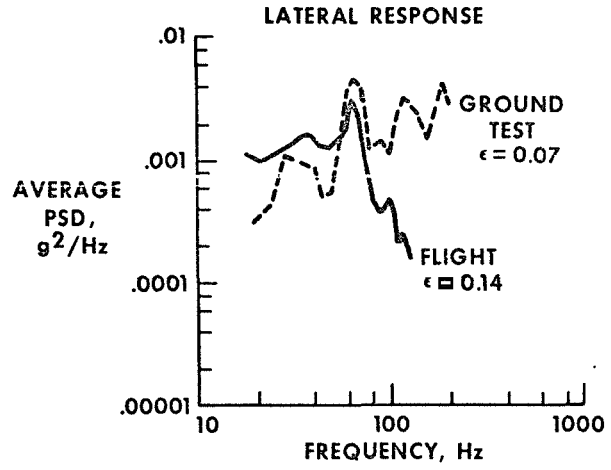

Figure 16. - Average vibration responses: Group D, lateral response (Y- and Z-axes) of tanks

excitation is approximately 6.3 psia, appreciably below the 14.7-psia ambient pressure of the earth at liftoff (Fig. 6). In addition, the decrease in static pressure also explains the low LM responses during this excitation: low joint acceptance of dynamic energy also prevails across the LM fluid/structure interface. Hence, low LM responses are a manifestation of this condition.

The PSD average of the flight and ground-test sound data (Fig. 18) shows that the LM excitations are generally similar; however, the two PSD's differ sufficiently to warrant adjusting (i.e., normalizing) the LM vibration PSD's to reduce uncertainty in comparisons of the vibration responses.

Normalized Vibration Responses

To provide the best directly comparable data, the PSD averages of Figs. 13 to 16 were normalized by ratioing the vibration PSD by the appropriate acoustic PSD of Fig. 18 (i.e., the flight-vibration PSD's were divided by the flight-acoustic PSD, etc.). This technique is fully developed by White [4] for prediction of SLA responses to various types of excitation. The resulting normalized spectra are then available for direct comparison, as plotted in Figs. 19 to 22.

EVALUATION OF RESULTS

Inspection of the normalized responses produced the following salient points:

1. The similarity of the ground-test and flight responses is limited. The best comparison occurs in the lateral motion of the secondary structure (Group B); however, even in this group, the ground-test response was much greater over most of the frequency range.

2. The masses of the ground-test and flight vehicles were nearly equal, both on an overall vehicle and on a component-by-component basis. However, above 100 Hz, the axial response of the flight LM's was an order of magnitude lower (Groups A and C).

3. At a frequency of 55 Hz, a stronger axial response occurred in flight than in the ground test.

4. The application of data for Groups C and D is limited by the relatively low cutoff frequency (110 Hz) of the flight data. Although ground test spectra are available to 2500 Hz, the plots for groups C and D were terminated at 200 Hz. This was done to preclude misleading interpretations which could possibly result from application of high-frequency (over 200 Hz) ground test data trends to extrapolation of the flight data. The other data (i.e., groups A and B) do not assure that the trends of the flight and ground test data will be similar above 200 Hz.

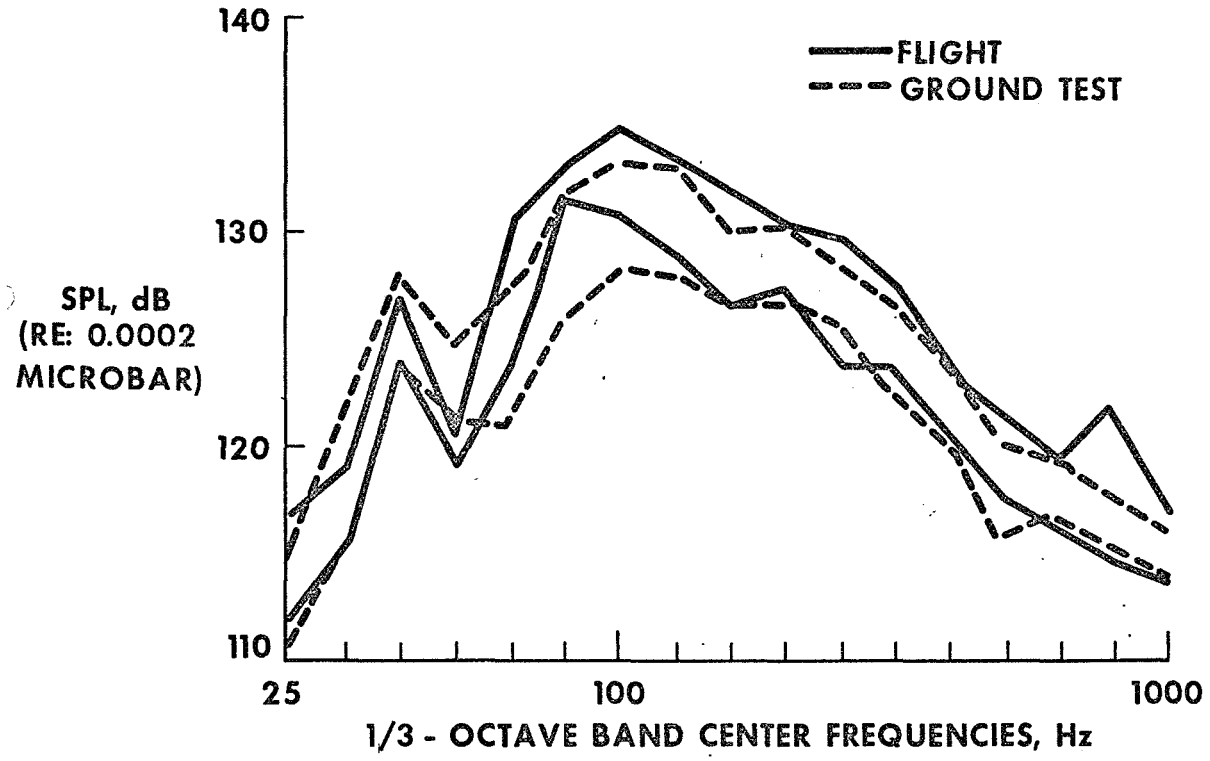

Figure 17. - Range of SPL inside SLA and external to LM

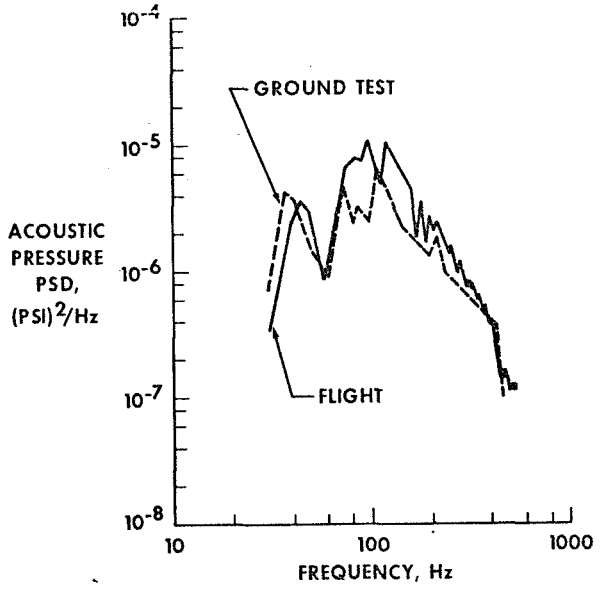

Figure 18. - Comparison of average acoustic pressure PSD's between the SLA and the LM

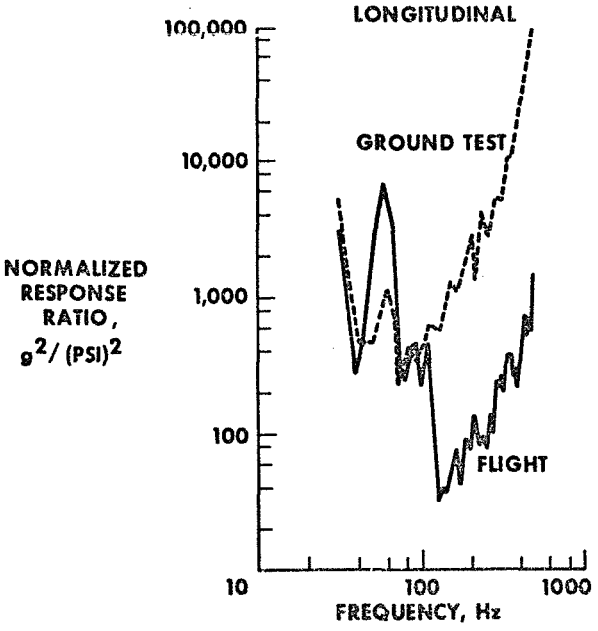

Figure 19. - Comparison of normalized LM response spectra: Group A, longitudinal response (X-axis) of secondary structure

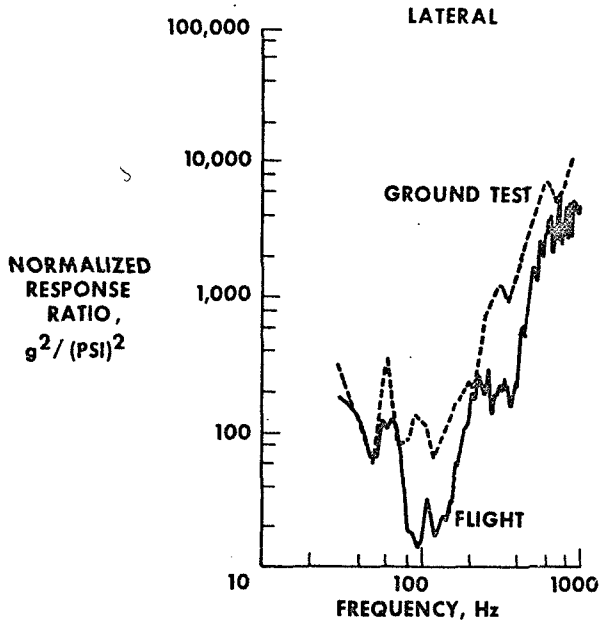

Figure 20. - Comparison of normalized LM response spectra: Group B, lateral response (Y- and Z-axes) of secondary structure

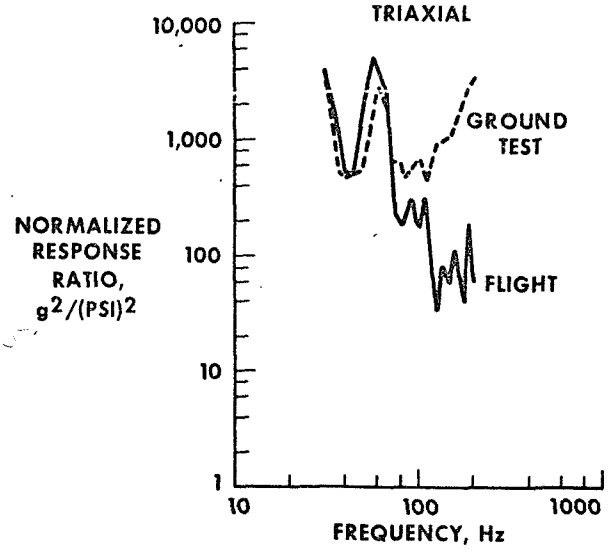

Figure 21. - Comparison of normalized LM response spectra: Group C, combined triaxial response of major mass items (tanks and descent-stage structure)

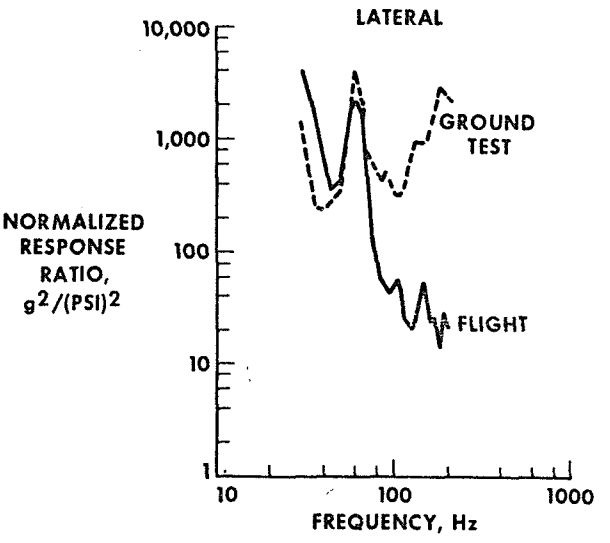

Figure 22. - Comparison of normalized LM response spectra: Group D, lateral response (Y- and Z-axes) of tanks

An appreciable difference between the flight and ground-test responses is thus found to exist. These differences can be attributed to two possible causes: (1) The flexibility and complexity of the LM structure is such that above 100 Hz, the dynamic responses may be highly dependent on the existing static load condition. The static loads were different between the launch and ground tests. (2) Several ambiguities occurred in both the ground and the flight tests. As a result, insufficient data are available on which to base a comprehensive assessment of acoustic excitation similarities.

The most significant ambiguities are as follows:

1. The flight vibration and acoustic measurements were not made on the same flights. Although the presumption that the acoustic field measured around LTA-2R and LTA-10R was the same as the sound field around LM-1 and LM-3 seems valid, the presumption cannot be quantitatively verified and is, therefore, unsupported.

2. The time slices for obtaining the flight vibration data were forced to be quite short by the time-sharing telemetry system, thus limiting the statistical reliability of the data. Also,

the number of statistically independent measurements is low if the orthogonal measurements on a triaxial installation are considered to produce only one independent measurement rather than three.

3. The narrow spectral range of many of the available flight measurements handicaps interpretation by truncating trends at a very low frequency.

4. The assumption of similar sound fields within the SLA for both the ground and flight tests is not clearly defensible. Although the structural similarities are manifold, insufficient data describing the sound fields in either test exist to support the assumption conclusively. Because phase-coherent instrumentation was not used in either test, the point-to-point correlation data (i.e., cospectra function) are not available. These data might have shown that large differences in the LM forcing function (internal SLA sound fields) existed between the ground and the flight tests.

Although LM instrumentation was adequate for the primary objective of the test programs (i.e., verification of the flightworthiness of the LM structure), two overriding limitations exist which definitely affect determining the fidelity of acoustic ground test simulation. First, flight instrumentation limitations severely curtail the quantity and usefulness of available data, and, second, the lack of phase-sensitive instrumentation in either flight or ground testing prevents reprocessing raw measurement records to obtain data regarding spatial characteristics of the acoustic field impinging on the LM. For these reasons, the uncertain consistency of the acoustic field coupled with the variability of LM responses precludes deliberate, detailed assessment of ground test simulation of flight environments.

RECOMMENDATIONS

The following recommendations (or observations) result from the comparison of the ground-test and flight data.

1. Careful control of test configurations and conditions is not in itself sufficient to assure comparable results between flight and ground tests.

2. Sufficient instrumentation for thoroughly measuring the vehicle environmental excitation and response must be used in the flight-test program to assure that ample data are available to support explanations for all observed phenomena (especially differences in responses).

3. The instrumentation used for environmental measurements (i.e., acoustic) must be phase coherent so that good cospectra data are available.

CONCLUDING REMARKS

The engineering development of the LM structure included an acoustic test program to verify structural adequacy to the fluctuating pressure environments that occur during launch. Vibration data from this testing and data obtained during the first two flights of the LM vehicle should have provided comparisons that indicated the degree of flight simulation obtained in the ground test. However, the comparisons available from the LM data are quite limited because of dissimilarities in the LM responses. These dissimilarities appear to result from the complexity of the LM structure and from measurement ambiguities. Since most of the ambiguities involve instrumentation limitations which can be avoided in future programs, a strong recommendation to recognize and prevent such limitations is a result of this comparative analysis.

REFERENCES

1. D. E. Newbrough, M. Bernstein, and E. F. Baird, "Development and Verification of the Apollo Lunar Module Vibration Test Requirements," Shock and Vibration Bull., No. 37, Part 5, pp. 105-115, Jan. 1968

2. W. D. Dorland, R. J. Wren, and K. McK. Eldred, "Development of Acoustic Test Conditions for Apollo Lunar Module Flight Qualification," Shock and Vibration Bull., No. 37, Part 5, pp. 139-152, Jan. 1968

3. J. S. Bendat and A. G. Piersol, Measurement and Analysis of Random Data. John Wiley & Sons, Inc., New York, 1966

4. R. W. White, "Theoretical Study of Acoustic Simulation of In-Flight Environments," Shock and Vibration Bull., No. 37, Part 5, pp. 55-75, Jan. 1968